CDF CENTRAL DETECTOR INSTALLATION: AN EFFICIENT MERGE OF DIGITAL PHOTOGRAMMETRY AND LASER TRACKER METROLOGY

John A. Greenwood and George J. Wojcik
Particle Physics Division: Alignment and Metrology Group
Fermi National Accelerator Laboratory, Batavia, Illinois, USA

1. ABSTRACT

Metrology for Run II at the Collider Detector at Fermilab (CDF) required a very complex geodetic survey. The Collision Hall network, surveyed with a Laser Tracker and digital level, provides a constraining network for the positioning of the Central Detector (CD). A part-based Laser Tracker network, which surrounded the 2,000-ton CD, was used as control for assembly. Subassembly surveys of the Detector's major components were measured as independent networks using Laser Tracker, V-STARS/S [1] digital photogrammetry system, and BETS [2] theodolite triangulation system. Each subassembly survey was transformed into and constrained by the part-based network. For roll-in, the CD part-based network was transformed into the Collision Hall network coordinate system. The CD was positioned in the Collision Hall using two Laser Trackers in "stakeout mode." This paper discusses the survey, adjustment, transformation, and precision of the various networks.

2. INTRODUCTION

This paper introduces the idea of combining networks measured using several different methods of surveying to develop the metrology for the CDF Run II experiment. The authors will discuss the strategy of measurements and adjustment of this complicated task.

3. NETWORK MEASUREMENTS AND ADJUSTMENT

This section will detail the survey and adjustment of local three-dimensional networks, established for purpose of alignment of the experiment's components.

3.1 Collision Hall network

The Collision Hall network was developed for the positioning of the CD, as well as monitoring local deformation. Figure 1 is a schematic view of the Collision Hall network, which contains both control and pass points, and indicates the complexity of the problem. Configuration of the points was established to optimally control the roll-in and final positioning of the CD.

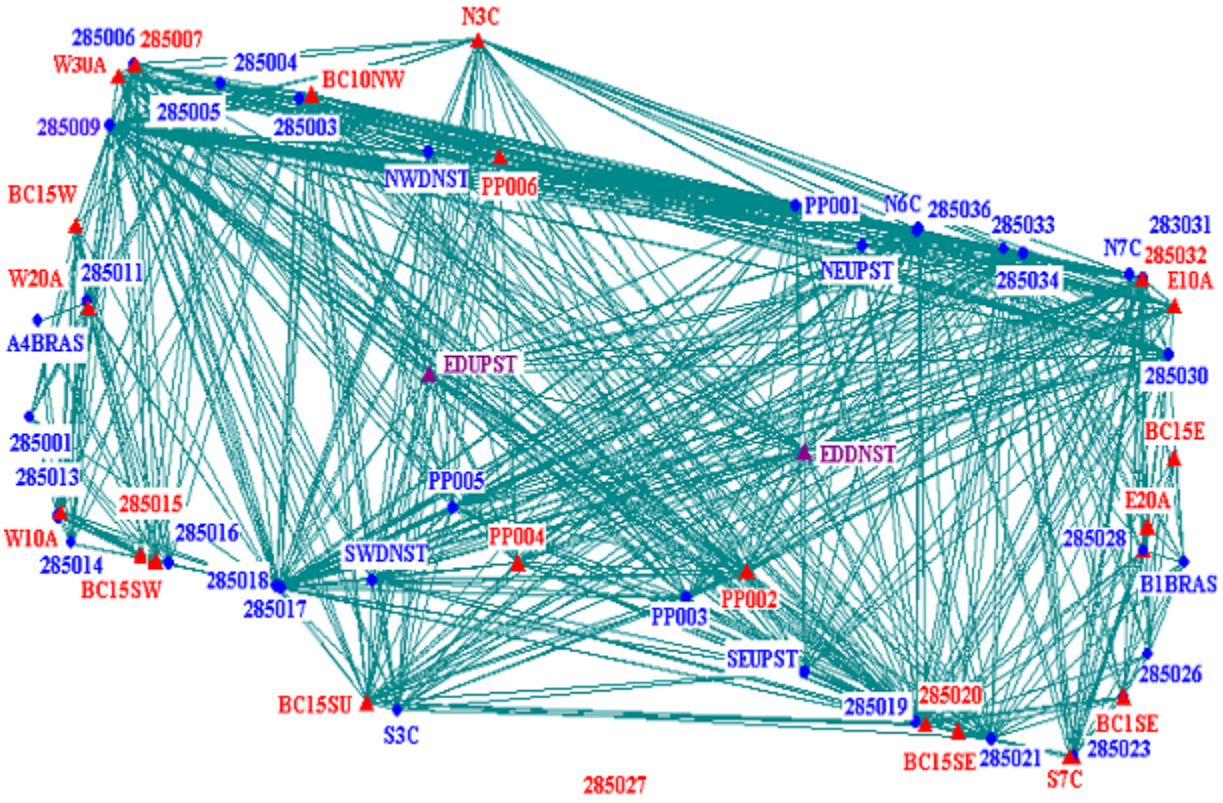

Figure 1 – Schematic view of Collision Hall Laser Tracker network

The Alignment and Metrology Group (AMG) at Fermilab performed the survey and adjustment of the Collision Hall network in December 1998 and January 1999. The SMX 4000 Laser Tracker (Figure 2**)** was used to perform a three-dimensional trilateration network in conjunction with a Leica NA3000 precise digital level.

Figure 2 - SMX4000 Laser Tracker

The observations made by the Laser Tracker are reported as 3-D coordinate values of the surveyed point. The LT 4000 was not used in a gravity-based coordinate system; instead, the internal head coordinate measuring system was used (Figure 3).

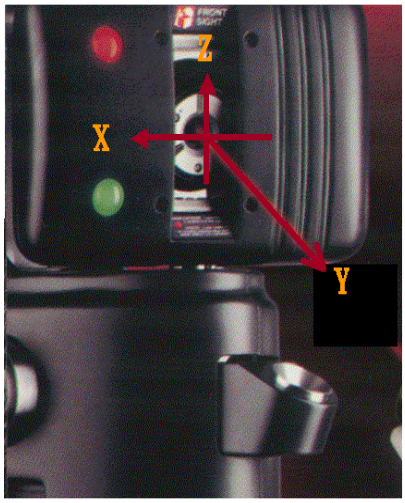

Figure 3 - Laser Tracker local coordinate system

The position of each point is determined from at least two stations. The coordinate data were used to generate weighted pseudo-slope distances, which in turn were used to compute the Collision Hall trilateration network. The vertical component of the network was reinforced by fixing on the adjusted elevations of 30 points. To maintain and update the DUSAF [3]

coordinate system, a minimally constrained adjustment of the horizontal network was chosen, fixed on one point, with the azimuth calculated from existing Collision Hall coordinates. Parameters of the adjustment and error propagation are shown in Tables 1, 2 and Figure 4.

Table 1 - Parameters of Collision Hall network adjustment

CDF COLLISION HALL ADJUSTMENT				
1STATISTICS SUMMARY				
NUMBER OBSERVATIONS		NUMBER UNKNOWNS		
HOR DIST				
SLOPE DIST	1034		ZERO ERRORS	0
DIRECTIONS	0		ORIENTATION	0
AZIMUTHS	1		ZENITH OFFSETS	0
COORDINATES	0		COORDINATES	177
TOTALS	1035			177
THE NUMBER OF DEGREES OF FREEDOM IS 858				
VARIANCE FACTOR FOR DISTANE	0.8252877			
COMBINED VARIANCE FACTOR	0.9945775			
CHI-SQUARE TEST ON THE VARIANCE FACTOR				
(VARIANCE FACTOR KNOWN)				
0.906786 < 1.000000 < 1.095836				
TEST OF VARIANCE FACTOR AT THE 95.000 % CONFIDENCE LEVEL PASSES				

Table 2- Example of error ellipses

1XY PLANE STATION 95.000 % CONFIDENCE ELLIPSES (METRES)
(VARIANCE FACTOR KNOWN) = 2..4484

NAME	a(m)	b(m)	°	‘	”
EDDNST	0.00002	0.00001	61	14	15
BC15W	0.00006	0.00004	32	07	50
BC15SE	0.00004	0.00004	281	02	43
BC15SU	0.00004	0.00002	282	00	35
BC15SW	0.00005	0.00004	351	34	19
285002	0.00004	0.00002	357	26	35
285006	0.00005	0.00002	352	43	00
285008	0.00005	0.00002	346	52	38

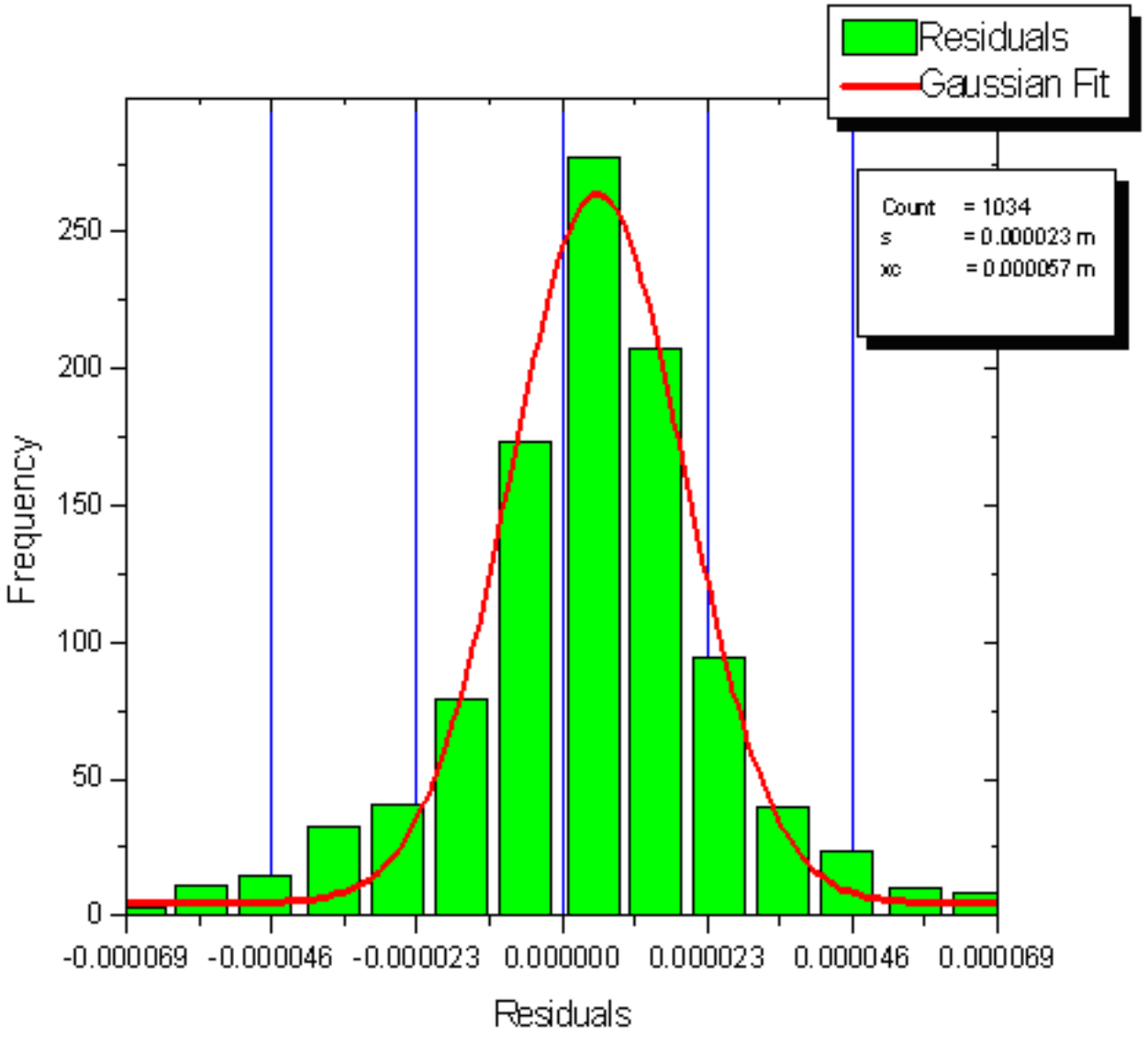

Figure 4 - Distribution of residuals with fit to Gaussian curve

Determination of Collision Hall deformation is very important in order to ensure the ongoing performance of the experiment. In the case of CDF, practical deformation determination could only be done by comparing offsets of eleven reference points from a common line (the survey in 1986 was performed using optical tooling methods) and offsets from the same points calculated in the recent adjustment. The strategy for the deformation analysis is shown in Figure 5.

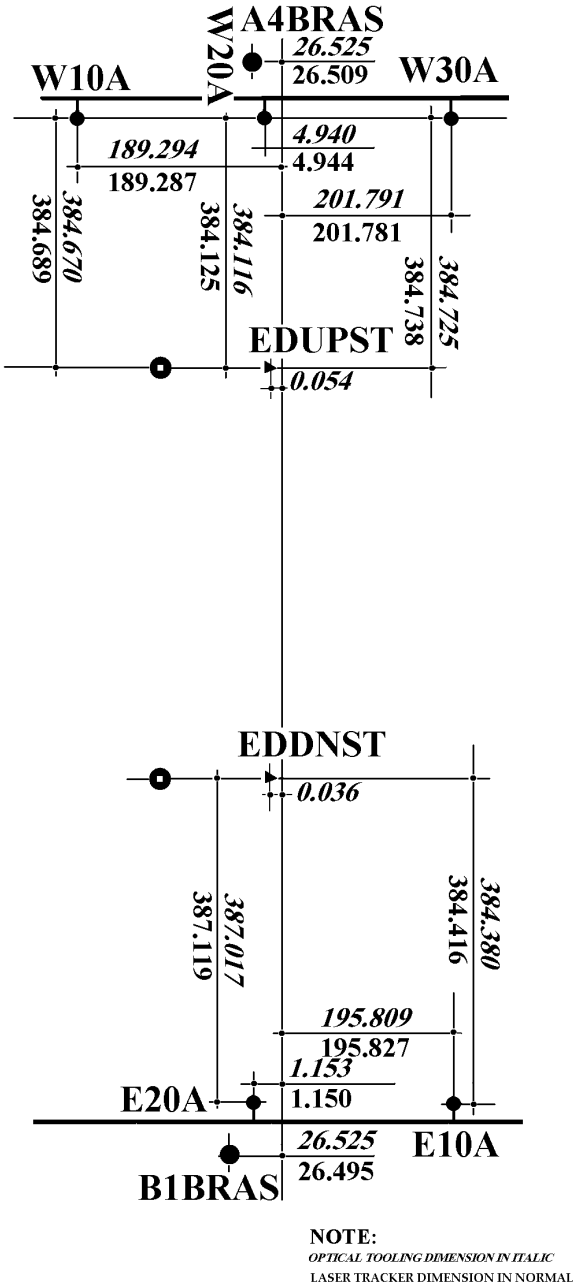

Figure 5 - Deformation analyzed by comparison of 1986 optical tooling survey with distances calculated from adjusted coordinates, expressed in inches.

3.2.1. Assembly Hall Laser Tracker Network

The Detector assembly hall network was much more complicated geometrically. The location of the Detector during assembly (Figure 6) required the creation of the Assembly Hall Laser Tracker (AHLT) network (Figure 7**)**. Targeting of the points, as well as the complexity of the Detector's components (Figure 9) required the use of many different measurement methods.

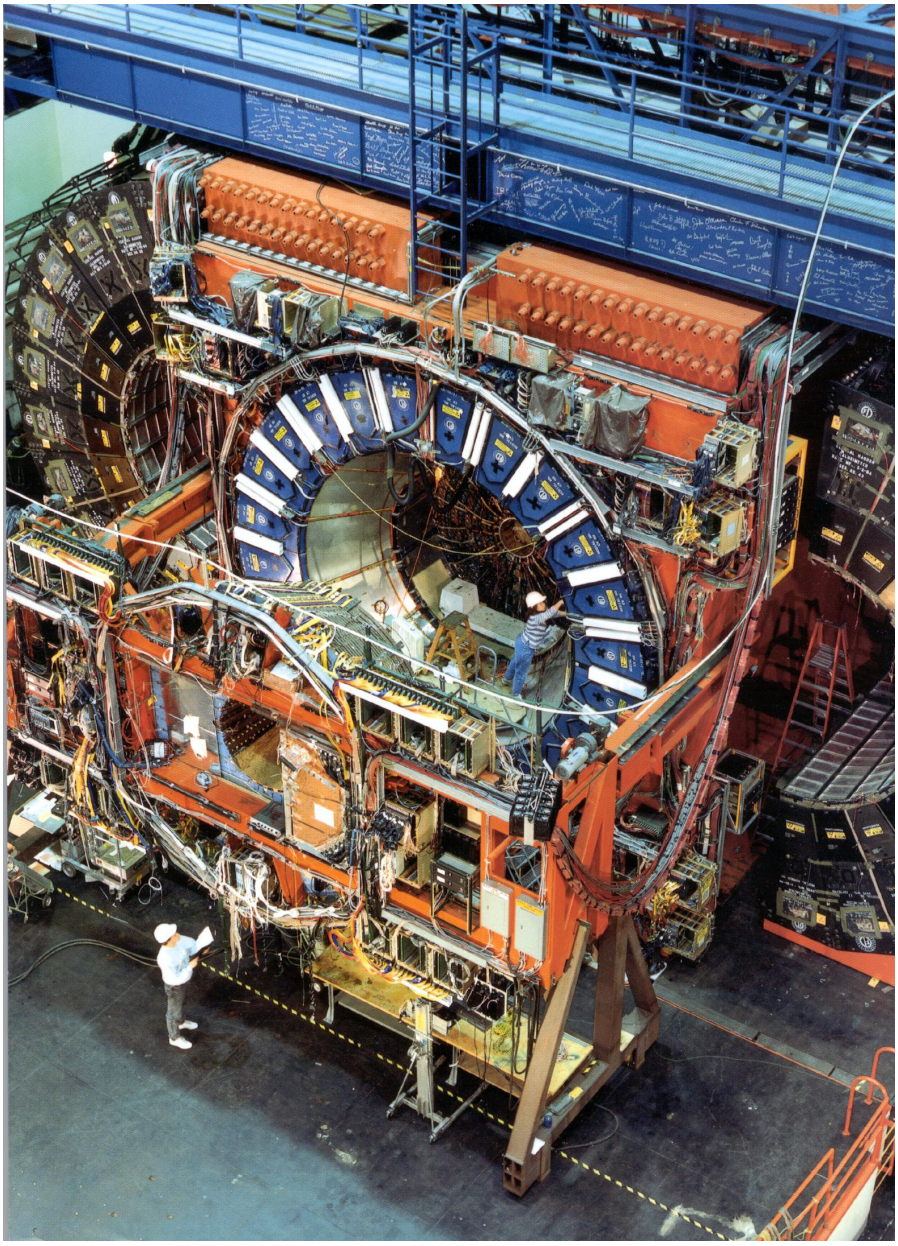

Figures 6 - View of West side of Central Detector

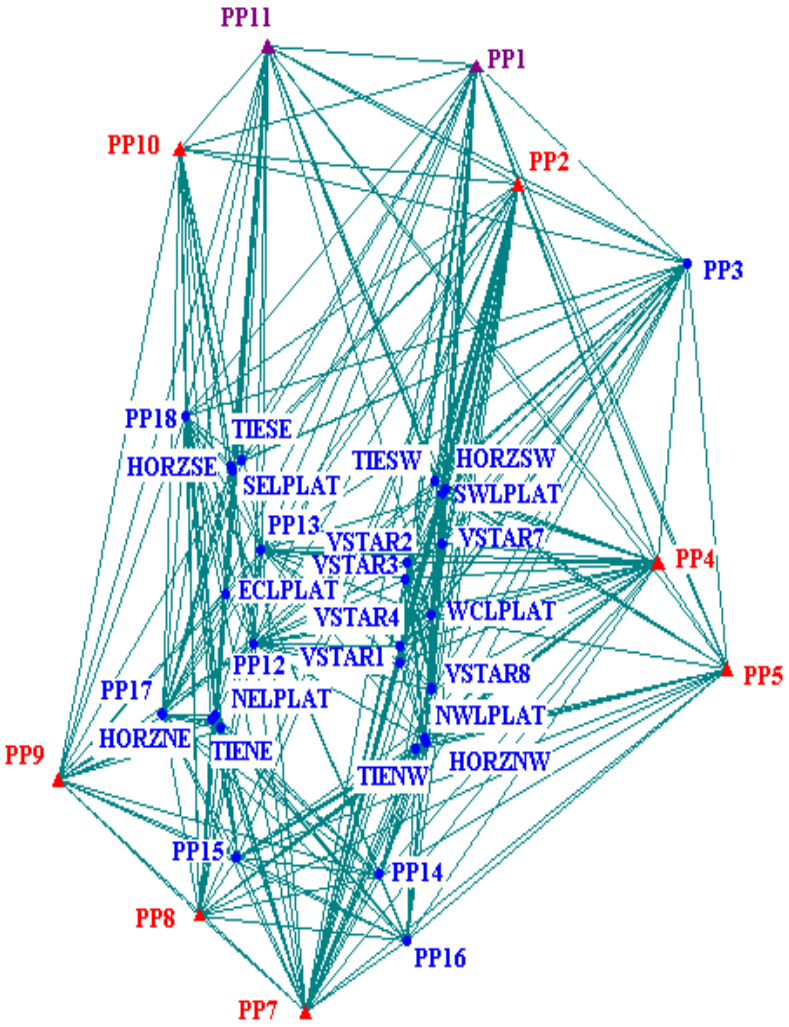

Figure 7 - Laser Tracker network in Assembly Hall

The six-station AHLT network survey was measured by the AMG in July 1999, using the SMX4000 Laser Tracker. Data reduction and adjustment of the AHLT network was similar to that of the Collision Hall network. Parameters of adjustments are shown in Tables 3, 4 and Figure 8.

Table 3 - Parameters of Assembly Hall network adjustment

CDF DETECTOR FINAL ADJUSTMENT LT IN THE GRAVITY SYSTEM				
1STATISTICS SUMMARY				
NUMBER OBSERVATIONS		NUMBER UNKNOW		
HOR DIST				
SLOPE DIST	343		ZERO ERRORS	0
DIRECTIONS	0		ORIENTATION	0
AZIMUTHS	0		ZENITH OFFSETS	0
COORDINATES	0		COORDINATES	104
TOTALS	343			104
THE NUMBER OF DEGREES OF FREEDOM 239				
VARIANCE FACTOR FOR DISTANE	0.7231424			
COMBINED VARIANCE FACTOR	1.0378153			
CHI-SQUARE TEST ON THE VARIANCE FACTOR				
(VARIANCE FACTOR KNOWN)				
0.874250 < 1.000000 < 1.252273				
TEST ON VARIANCE FACTOR AT THE 95.000 % CONFIDENCE LEVEL PASSES				
(0 RESIDUALS WERE FLAGGED FOR REJECTION)				

Table 4 - Example of error ellipses

1XY PLANE STATION 95.000 % CONFIDENCE ELLIPSES (METRES)
(VARIANCE FACTOR KNOWN) = 2..4484

NAME	a(m)	b(m)	º	‘	”
TIESW	0.00017	0.00011	3	29	44
HORZSW	0.00011	0.00010	1	34	59
SWLPLAT	0.00013	0.00010	45	04	27
WCLPLAT	0.00013	0.00010	78	33	27
VSTAR1	0.00014	0.00011	68	05	03
VSTAR8	0.00014	0.00011	73	15	26
PP12	0.00013	0.00011	60	51	49
NWLPLAT	0.00015	0.00011	74	42	08

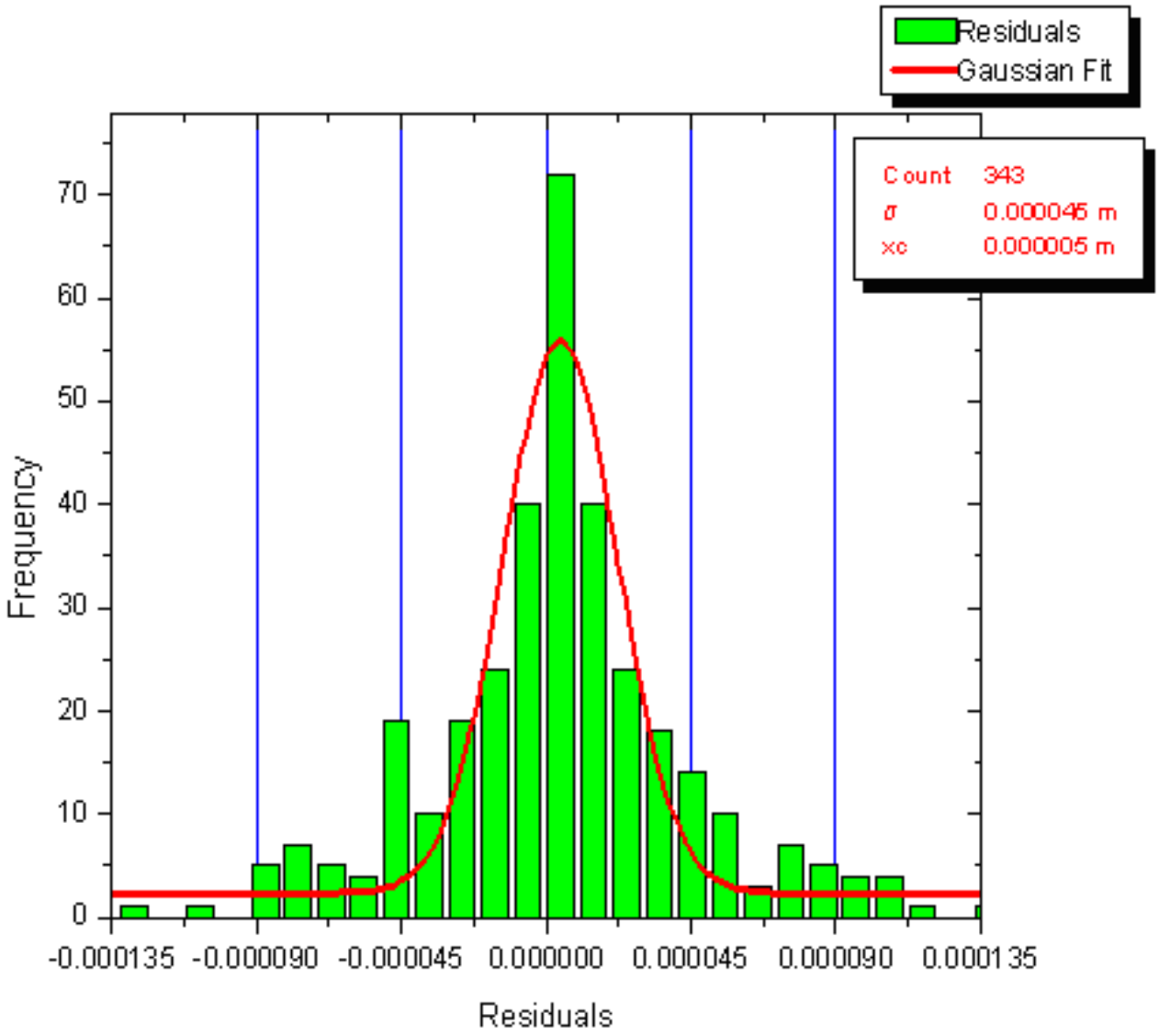

Figure 8 - Distribution of residuals with fit to Gaussian curve

Adjusted coordinates of the AHLT network points were used as control for the best-fit transformation of coordinates from the BETS theodolite triangulation data. Tables 5, 6, 7, and 8 show the strategy and results of these transformations.

Table 5 - Coordinates of master points for transformation

FILE WEST.NEW			
(A6,3(F15.7))	X(m)	Y(m)	Z(m)
SWLPLA	-0.73634	-3.23845	-1.40351
WCLPLA	-1.13717	-6.72247	-1.39701
NWLPLA	-1.37753	-10.24353	-1.39768
PP5	9.03315	-8.22385	-0.03261

Table 6 - Coordinates of BETS points to transform

FILE WEST.OLD			
(A6,3(F15.7))	X(m)	Y(m)	Z(m)
X0-1	4.42619	7.21859	6.20589
X0-2	4.42548	7.21902	6.19776
X0-3	4.42609	7.21887	6.19266
X0-4	4.41864	7.22611	-1.03945
X0-5	4.41864	7.22596	-1.04867
X0-6	4.41857	7.22619	-1.05682
Z0-1	0.64054	6.86480	2.53409
Z0-2	0.65616	6.86607	2.53424
Z0-3	0.67005	6.86713	2.53442
Z0-4	0.68458	6.86883	2.53345
Z0-5	7.89721	7.54930	2.52827
Z0-6	7.90630	7.54994	2.52824
Z0-7	8.20691	7.64877	2.55306
SWLPLA	-0.73618	-3.23866	-1.40352
NWLPLA	0.91857	6.77739	-1.23998
WCLPLA	4.42416	7.18649	-1.23909
PP5	4.81283	-3.08702	0.12532

Table 7 - Results of transformation for best-fit of four BETS points

```
                        PROGRAM CHABA
   ************************************************************************
   *                                                                      *
   *     FILE WEST.NEW                                                    *
   *                                                                      *
   ************************************************************************
   REJECTION TOLERANCE FOR THE ACTIVE POINTS    1.00000
   TRANSFORMATION DATA   Xnew = S * Ry * Rx * Rz * Xold + Xo
   ************************************************************************************
   *TERMS OF ROTATION MATRIX (Phi,Omega,Kappa)                                        *
   *  P1  =   0.1833332634  P2  =  -0.9830508199  P3  =   0.0000070856          *
   *  Q1  =   0.9830508194  Q2  =   0.1833332635  Q3  =   0.0000304286          *
   *  R1  =  -0.0000312119  R2  =   0.0000013870  R3  =   0.9999999995          *
   *          ANGLES OF ROTATION                                                *
   *  KAPPA (Z AXIS) =    88.262251640  (ESTIMATED)                            *
   *  OMEGA (X AXIS) =     0.001937143  (ESTIMATED)                            *
   *  PHI   (Y AXIS) =   399.999548914  (ESTIMATED)                            *
   *          SCALE FACTOR                                                      *
   *  Sxyz =    0.9999803683  (ESTIMATED)                                       *
   *          TRANSLATION VECTOR                                                *
   *  Xo  =      -3.073975 (EST) Yo  =     -11.684025 (EST) Zo  =   -0.157880 (EST) *
   ************************************************************************************

                       COORDINATES OF ACTIVE POINTS

      NEW      SYSTEM                              OLD     SYSTEM
  NOM       X             Y             Z          X             Y             Z
SWLPLA    -0.73634      -3.23845      -1.40351      7.92245       7.43094      -1.24554
WCLPLA    -1.13717      -6.72247      -1.39701      4.42416       7.18649      -1.23909
NWLPLA    -1.37753     -10.24353      -1.39768      0.91857       6.77739      -1.23998
PP5        9.03315      -8.22385      -0.03261      4.81283      -3.08702       0.12532

  ADJUSTED COORDINATES OF ACTIVE POINTS FROM OLD SYSTEM TO NEW SYSTEM

  NOM            X             Y             Z        DX(mm)   DY(mm)   DZ(mm)   DD(mm)
SWLPLA         -0.73618      -3.23866      -1.40352    0.16    -0.21    -0.01     0.27
WCLPLA         -1.13721      -6.72240      -1.39696   -0.04     0.07     0.05     0.10
NWLPLA         -1.37773     -10.24351      -1.39774   -0.20     0.02    -0.06     0.21
PP5             9.03323      -8.22373      -0.03260    0.08     0.12     0.01     0.15

           ***  EMQ DD = 0.19  ***
```

Table 8 - Results of transformation for best-fit of three BETS points

```
                        PROGRAM CHABA
    ************************************************************************
    *                                                                      *
    *     FILE WEST.NEW                                                    *
    *                                                                      *
    ************************************************************************
    REJECTION TOLERANCE FOR THE ACTIVE POINTS    0.1
    TRANSFORMATION DATA   Xnew = S * Ry * Rx * Rz * Xold + Xo
    ********************************************************************************
    *TERMS OF ROTATION MATRIX (Phi,Omega,Kappa)                                    *
    *  P1  =   0.1833392779  P2  =  -0.9830496982  P3  =   0.0000050272          *
    *  Q1  =   0.9830496967  Q2  =   0.1833392779  Q3  =   0.0000553773          *
    *  R1  =  -0.0000553604  R2  =  -0.0000052108  R3  =   0.9999999985          *
    *          ANGLES OF ROTATION                                                *
    *  KAPPA (Z AXIS) =    88.261862134  (ESTIMATED)                            *
    *  OMEGA (X AXIS) =     0.003525431  (ESTIMATED)                            *
    *  PHI   (Y AXIS) =   399.999679958  (ESTIMATED)                            *
    *          SCALE FACTOR                                                      *
    *  Sxyz =    0.9999604328  (ESTIMATED)                                       *
    *          TRANSLATION VECTOR                                                *
    *  Xo  =      -1.212370 (EST) Yo  =     -12.022237 (EST) Zo  =   -0.157850 (EST) *
    ********************************************************************************

              COORDINATES OF ACTIVE POINTS


                  NEW      SYSTEM                              OLD     SYSTEM
  NOM      X             Y             Z             X             Y             Z
WCLPLA   -1.13717      -6.72247      -1.39701       4.42416       7.18649      -1.23909
NWLPLA   -1.37753     -10.24353      -1.39768       0.91857       6.77739      -1.23998
PP5       9.03315      -8.22385      -0.03261       4.81283      -3.08702       0.12532

  ADJUSTED COORDINATES OF ACTIVE POINTS FROM OLD SYSTEM TO NEW SYSTEM

  NOM            X             Y             Z         DX(mm)   DY(mm)   DZ(mm)   DD(mm)
WCLPLA         -1.13708       -6.72250      -1.39700     0.09    -0.03     0.01     0.09
NWLPLA         -1.37762      -10.24353      -1.39769    -0.09     0.00    -0.01     0.09
PP5             9.03315       -8.22382      -0.03261     0.00     0.03     0.00     0.03


      ***  EMQ DD = 0.08  ***


 COORDINATES OF PASSIVE POINTS IN NEW SYSTEM

 NOM              X             Y             Z
X0-1            -1.16823       -6.71421       6.04769
X0-2            -1.16878       -6.71483       6.03956
X0-3            -1.16852       -6.71425       6.03446
X0-4            -1.17704       -6.72065      -1.19737
X0-5            -1.17689       -6.72068      -1.20659
X0-6            -1.17713       -6.72070      -1.21474
Z0-1            -1.51450      -10.50060       2.37624
Z0-2            -1.51288      -10.48502       2.37639
Z0-3            -1.51138      -10.47117       2.37657
Z0-4            -1.51038      -10.45657       2.37560
Z0-5            -0.85699       -3.24173       2.37002
Z0-6            -0.85595       -3.23268       2.36999
Z0-7            -0.89799       -2.91905       2.39479
```

Coordinates of the final BETS points were transformed into the AHLT reference frame. Additional Laser Tracker points were observed in the AHLT to support the V-STARS data adjustment. Parametric adjustment of the Laser Tracker data provided error propagation information in the form of standard errors of the adjusted points. The V-STARS bundle ray adjustment was constrained on several Laser Tracker points and weighted according to errors in coordinates, δ_x, δ_y , δ_z, as shown in the example covariance matrix in Table 9.

Table 9 - Example of error propagation covariance matrix and errors of coordinates

########## **VSTAR1** ##########

X (COL 1)	Y (COL 2)	Z (COL 3)
0.32204899D-08	-0.16823831D-09	0.47594594D-09
-0.16823831D-09	0.52555409D-09	0.23431397D-09
0.47594594D-09	0.23431397D-09	0.22289915D-08

δ_x = +/- 0.00014 m, δ_y = +/- 0.00006 m, δ_z = +/- 0.00012 m

########## **VSTAR2** ##########

X (COL 1)	Y (COL 2)	Z (COL 3)
0.26732258D-08	-0.22047265D-09	0.53039785D-09
-0.22047265D-09	0.54869861D-09	-0.68765626D-10
0.53039785D-09	-0.68765626D-10	0.20936728D-08

δ_x = +/- 0.00013 m, δ_y = +/- 0.00006 m, δ_z = +/- 0.00011 m

3.2.2. Assembly Hall Theodolite Triangulation

BETS theodolite triangulation system was used to obtain coordinates of points with punch mark signalization on the east and west faces of the CD, which were used during Run I construction.

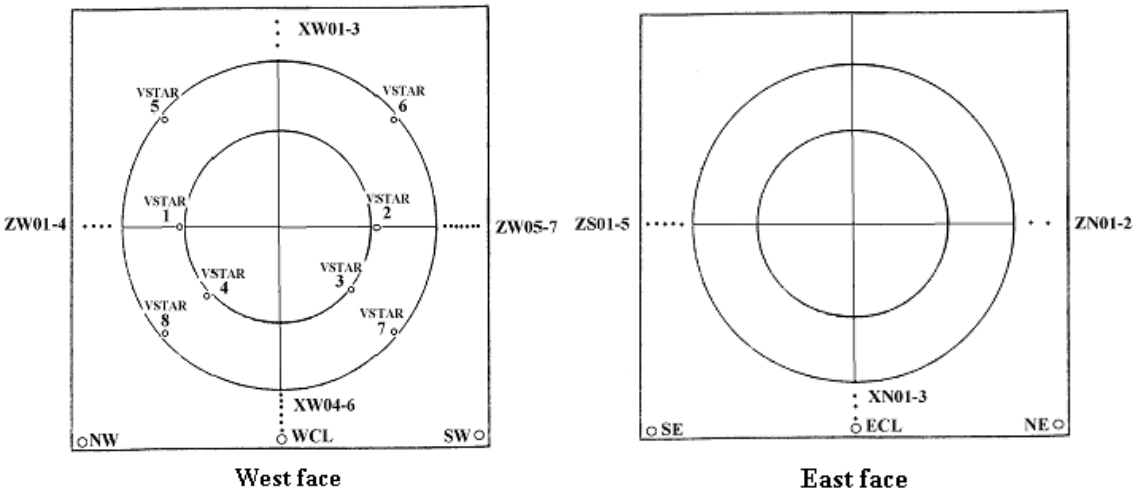

Figure 9 - Schematic view of signalization points of BETS and V-STARS

3.2.3. Assembly Hall Photogrammetry

The V-STARS digital photogrammetry system was used because of its inherent accuracy, speed, and efficiency when measuring the very detailed areas inside the Detector. A major benefit of using photogrammetry, when compared to other precision systems, is that it does not require a stable platform from which to operate. This was of particular value when working at the higher levels, such as the solenoid bore 6m above the floor, from scaffolding or using a man-lift. (Figures 10 and 11)

The photogrammetric surveys undertaken in this effort fall into two principal categories:

1) Measurement efforts of separately supported systems
2) Measurement of components directly supported by CD or spaces within the CD

The bulk of the effort falls within Category 2), however, the separately supported systems listed in Category 1) do, nonetheless, represent in their own right, very major efforts.

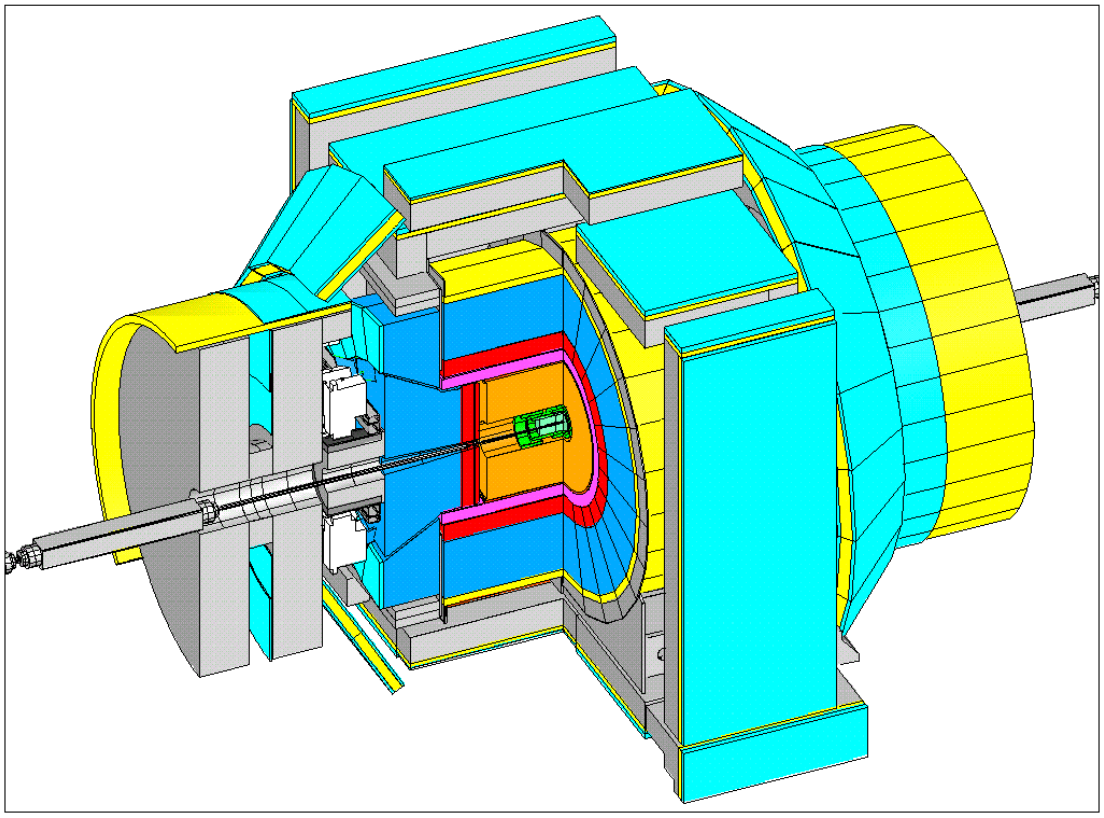

Figure 10 - Central Detector isometric

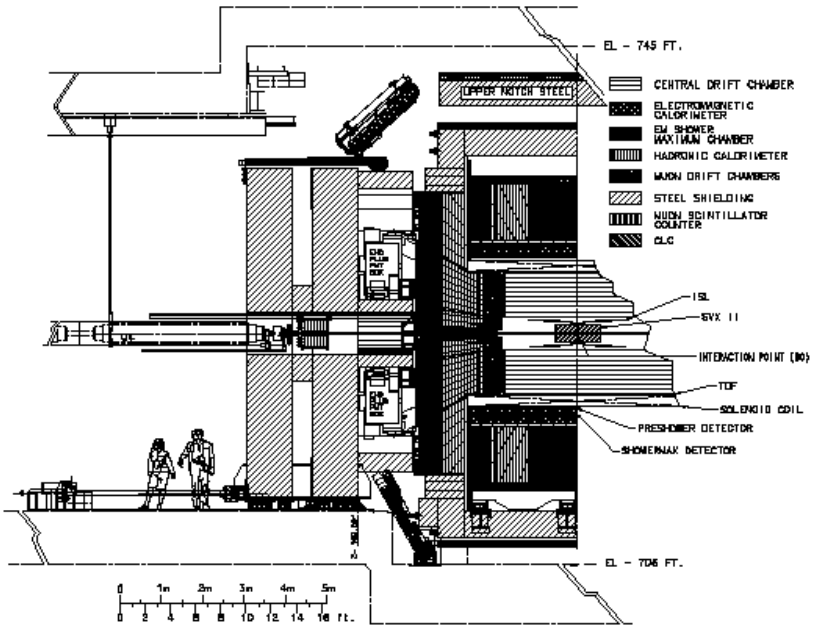

Figure 11 - Central Detector section

3.2.3.1 Category 1 photogrammetry

1. The Run I toroids were recommissioned as shielding and as a carrier for the muon detection system, now known as Muon Steel
2. Cosmic ray detectors
3. End Plugs and supporting framework
4. Central Outer Tracker (COT) assembly
5. VTX/SVX (Run I system) extraction sled path mapping
6. Feature target referencing for COT and Time-Of-Flight (TOF) systems
7. Cherenkov Luminosity Counter (CLC) design survey
8. Intermediate Silicon Layer (ISL) inchworm calibration

3.2.3.1.1 Muon steel

The toroids from Run I were modified to act as shielding steel and as the support structure for a portion of the intermediate muon detection system (IMU). The two structures are formed as a pair of two half-cylinders, one system on each side of the CD, with a nominal radius of 3.8m and 4.0m in length (Figure 12). The task was to determine the smallest cylinder that could be constructed on the circumferential surfaces, relative to the beam line, the parallelism of the mating surfaces, and the perpendicularity of the ends. Thirty-four L-shaped vector targets, with a magnetic foot, were fabricated for the surface mapping of each of the toroid segments (Figure 13.). The targets were set at the local high-points along a 0.5m wide circumferential band,

photographed from a man-lift, then moved to the next band. The ends and mating faces were targeted using retro-reflective adhesive 6mm targets. Each half-cylinder segment required approximately 200 exposures.

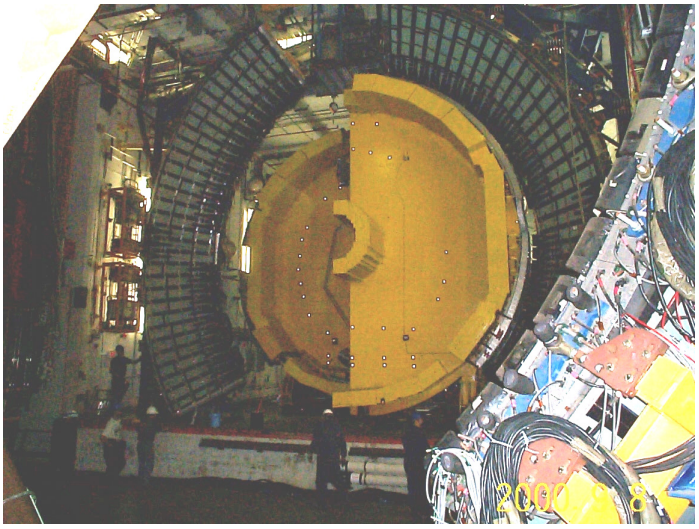

Figure 12 – Muon steel at full stagger

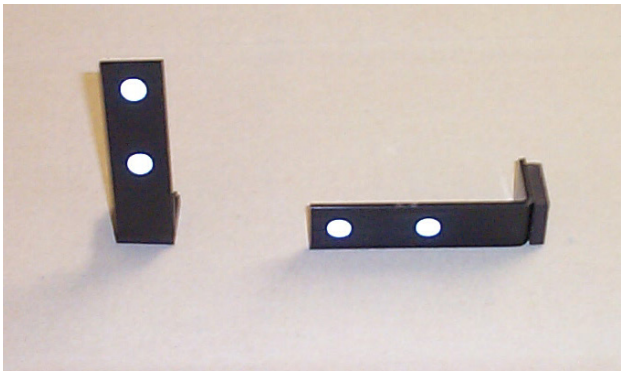

Figure 13 – Muon steel vector targets

3.2.3.1.2 Cosmic ray detectors

The cosmic ray detector system is a series of rectangular aluminum boxes with orthogonal wire planes inside. The only exposed features are the pins on the connectors. A set of adapters was made that could be placed on the pins on each end of the connector, and accept a 0.125-inch post tooling target. The fiducials were 0.250-inch bushings into which were placed 6mm tooling targets with 0.500-inch offset, corresponding to the offset of the tooling balls planned for installation. Lines connecting the wire ends from opposite sides were constructed in the chamber reference frame.

3.2.3.1.3 End plugs

The end plugs are large objects resembling the nose cone of an Apollo spacecraft. They are supported by external structures that allow them to be removed for access to the solenoid bore of the CD. The beam pipe passes through a 3° axial hole. The task was to determine parallelism of the two faces, determine the direction and position of the axial hole, and fiducialize the support structure.

3.2.3.1.4 COT assembly

The COT is an aluminum cylindrical chamber with a diameter of 3m and a length of 3m. The end plates are 41.275mm thick, with more than 5000 circuit board slots machined in each end, with a 1m diameter central hole, which attaches to a carbon fiber support tube. Each end plate has a series of survey holes on the face, ten at the outer edge, six intermediate holes, and six inner holes. The task was to place the end plates at the prescribed separation, parallelism, and clocking. This was done using the Laser Tracker to establish the end-to-end control, then measuring the clocking with photogrammetry. Because the end plates contain all the electronic connections, about 15cm deep, a set of feature targets (3.2.3.1.6) were fabricated and referenced for the outer survey holes (Figures 15 and 16.). Several repeat surveys were made of the end plates to determine the amount of distortion caused by the loading and tensioning of the wire strips.

3.2.3.1.5 VTX/SVX extraction

The VTX and SVX are Run I components being replaced as part of the upgrade. As part of the disassembly of the Run I configuration, these components needed to be extracted without damaging the beryllium beam pipe. The original insertion sled needed to be refurbished and aligned. The sled rides on rails and has an extendable attachment fixture. The tracking of the attachment fixture, relative to the sled rails, was measured using photogrammetry.

3.2.3.1.6 COT and TOF Feature targets

Feature targets are specially constructed fixtures that permit the measurement of abstract features. A coded target (Figure 14), which has a central circular index feature and seven square, uniquely located identifier features arranged in a two-dimensional array, when attached to a suitable interface, becomes capable of measuring properties of object features. The software recognizes the identity of the coded target by the spatial relationship of the seven square features known as nuggets. The eight objects provide a unique data set with more than enough inherent information to establish a local reference frame for the fixture. If the coded target is placed on some artifact that contains an interface to a feature, the eight coded target objects may be referenced to that interface, thereby creating a datum reference frame abstraction. Once the relationship between the coded target objects, the fixture reference frame origin, along with any other pertinent features is known, the fixture is placed in an object space scene attached to a suitable feature.

During the processing phase, a template file for each feature target is imported, which contains the coded target objects and such other related features as may be pertinent. At the conclusion of the bundle adjustment phase of processing, the features contained in the template reference frame are transformed into object space reference frame. This yields the coordinate location and/or feature orientation in the object reference frame.

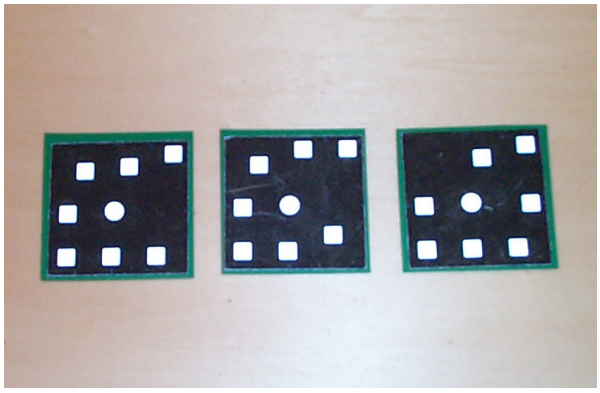

Figure 14 - Coded targets

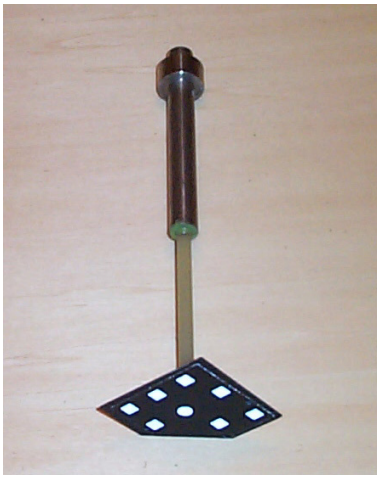

Figure 15 - COT Feature target

The COT feature target (Figure 15) attaches to an outer survey hole at the machined end (top of Figure 15). This particular feature target indicates the coordinates of the survey hole at the face of the end plate and the pitch and yaw of the hole. Ten such targets were fabricated, one for each hole (Figure 16). When in use, a specific target is associated with a specific survey hole to facilitate differential measurements.

Figure 16 - COT Feature targets

The TOF feature targets were fabricated from 36 photo multiplier tube (PMT) housing end caps. Small adhesive coded targets were placed on the end caps. A reference fixture was constructed using the PMT housings. See section 3.2.3.2.4.

3.2.3.1.7 CLC

The CLC are long conical shaped devices, which lie within the 3° axial hole of the end plugs. The 3° hole is not a conical feature, but a series of stepped, concentric rings welded in a stack, thus producing a conically limited aperture. The suitability of this volume is further limited by the beam pipe axis and the requirement that the CLC be as concentric to the beam pipe as possible. This feature was mapped using the Laser Tracker.

3.2.3.1.8 ISL inchworms

The Intermediate Silicon Layer carrier is a component of the active alignment system. It is designed to make small moves of the carrier using devices known as inchworm actuators. An inchworm has the capability of moving in discrete steps of approximately 1 micron over a range of approximately 1500 steps. The difficulty in using these devices is that from one unit to the next the steps are only approximately equal in size. The carrier uses five inchworms, three placed at 120° intervals around the circumference of one end (top, lower left, lower right) and two on the other end (lower left, lower right, but with a floating positioning device at the top). By moving the five inchworms in combination, translations laterally and vertically, along with roll, pitch, and yaw maneuvers, can be accomplished. Since each inchworm has a slightly different step size, the system needed to be calibrated and cross-talk studied. This was done with the carrier installed on a long granite table, targeted on each end using coded targets, adhesive targets, and precision ¼”-hole construction plates with tooling targets, then using photogrammetry to measure changes in the end ring positions after each series of inchworm moves. A baseline set of measurements was made to establish the positions with all inchworms at a nominal setting, and to tie the two ends together in a common reference frame. Once the baseline measurements were completed, an additional 48 sets of measurements were taken after inchworm moves were made, eighteen exposures on each end for each set.

3.2.3.2 Category 2 photogrammetry

1. Survey from the AHLT control on the east face of the CD, through the solenoid bore, to AHLT control on the west face of the CD
2. VTX/SVX extraction
3. Survey of the CD solenoid bore for design parameters of the TOF system
4. TOF system positioning in solenoid bore
5. COT positioning
6. ISL positioning
7. Beam pipe location
8. End plug placement surveys

3.2.3.2.1 Photogrammetric connection of east and face faces, through the solenoid

Figure 6 shows the west face of the CD in what appears to be a reasonably spacious environment. In contrast, the east face is very cramped, barely allowing a man-lift to traverse the face. As such, when the AHLT survey was being performed, the control measurements on the east face were limited to the lower part of the CD. Since the positioning of components near the beam axis of the CD requires the utmost precision, and, oftentimes, requires many repeat measurements, it is very useful to have precise control in the proximity of the solenoid bore ends. A series of construction plates were placed at the inner and outer margins of the 30° end plug mating surface (Figures 6, 10, and 11) on each face. The construction plates were measured using the Laser Tracker on the west end, but could not be observed on the east end.

The construction plates offer a convenient targeting interface between the Laser Tracker surveys and the photogrammetric surveys. The spherically mounted reflector (SMR) and adapter nest of the Laser Tracker provides a measurement point one-inch above the plate surface, on the axis of the ¼" mating hole (+/- 0.0005" – 12.7μm – in all directions). Photogrammetric tooling targets are manufactured with the same interface, offset, and tolerances, but are available with a reflective dot placed on angles of 0°, 45°, and 90° (Figure 17).

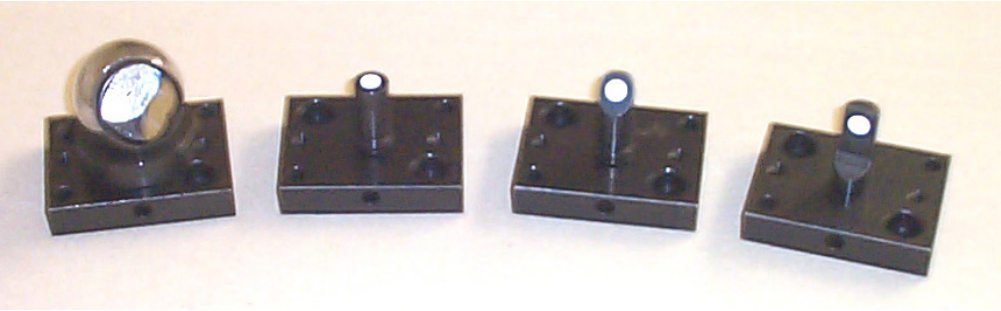

Figure 17 – 1" offset SMR and photogrammetric targets

A photogrammetric survey, comprised of 215 images, was tied to the AHLT control on the east face, advanced up the east face, connecting the construction plates on the east 30° mating surface, through the 3m diameter solenoid bore, connecting the construction plates on the west 30° mating surface, then tying to the AHLT control on the west face. The details of the precision of this survey are described in Section 4.

3.2.3.2.2 VTX/SVX Extraction

As described in 3.2.3.1.5, the VTX and SVX systems from Run I required removal using an extraction sled that had been aligned for this purpose. For the actual removal process, the sled was placed on top of a stack of concrete blocks, and then oriented such that the extraction axis was coaxial with the beam pipe. This task required photogrammetry, Laser Tracker, and optical tooling measurements.

3.2.3.2.3 Solenoid bore mapping

The solenoid bore is a 3m diameter aperture that extends from the inner limits of the 30° mating surfaces. It acts as, among other things, the support structure for the TOF system. The TOF system is comprised of a series of seventy-two PMT-triplets at each end. A series of ledges establish the position of these devices. The design issue was to determine the largest available coaxial cylinder (largest outer diameter and smallest inner diameter, concentric with the beam axis) within the solenoid bore and outside the extent of the COT. The solenoid bore surface is not a machined surface, having several welding seams and other surface irregularities caused by the original forming of this piece. These measurements were made using the Laser Tracker, acquiring more than 15,000 points on the solenoid bore surface, using a pattern of parallel rings and following the welding features and local anomalies.

A best-fit maximum cylinder was determined in the AHLT reference frame. The axis of this cylinder then served as the new CD beam axis, moving the Run I reference frame by approximately 2mm, as defined by the punch marks shown in Figure 9.

Once the TOF beneficial volume was determined, the ledges were designed, fabricated, and installed. Installation verification was done by placing adhesive photogrammetric targets on the inner extent of the TOF ledges.

3.2.3.2.4 TOF installation

The TOF system is comprised of 216 three-meter long scintillator bars with a PMT on each end, supported by the ledges described in 3.2.3.2.3 and the PMT housings described in 3.2.3.1.6. The central coordinate and the axis of each housing, on each end, had to be determined. This was done using the feature targets described in 3.2.3.1.6, sequencing the set of 36 targets in six segments around the array, on each end.

3.2.3.2.5 COT positioning

The COT is supported at each end by a pair of brackets at the horizon. The brackets are attached to supports near the horizon of the CD. Both ends of the COT were measured, the best-fit central axis and horizon calculated, and then compared to the beam axis and horizon of the CD, in order to determine the position adjustments. The COT was positioned photogrammetrically using feature targets described in 3.2.3.1.6 and the control described in 3.2.3.2.1. Normally photogrammetry is not a suitable stakeout technique, but in this case, the advantage of not requiring a stable platform from which to operate overrode the disadvantage of multiple measurement iterations.

Figure 18 – COT insertion with TOF on solenoid bore

3.2.3.2.6 ISL positioning

The ISL is mounted in the central bore of the COT. Again, for the reasons described in 3.2.3.2.5, photogrammetry was used. The difference between ISL and COT positioning tasks is because the ISL is an active alignment device, driven by the inchworms described in 3.2.3.1.8. It was first necessary to mechanically center the ISL, and then adjust the five inchworms to the center of travel, followed by several iterations of movement-readout confirmation.

3.2.3.2.7 Beam pipe location

The beam pipe was positioned using the control system of 3.2.3.2.1 and conventional photogrammetric tooling targets mounted in special adapters installed on the beam pipe flange. Initial adjustment was done using stic micrometer measurements, followed by photogrammetry for confirmation.

3.2.3.2.8 End plug placement surveys

The end plugs are not critically aligned, but knowledge of the orientation relative to the CD beam axis and horizon is required. The end plug support framework carries a series of construction plates (Figure 19), while the CD has a companion set of construction plates which, when the end plugs are in the closed position, are in close proximity. The construction plates may be targeted with either photogrammetric tooling targets or Laser Tracker SMR targets (Figure 17), depending on the measurement situation. Because the end plugs must be withdrawn to service the solenoid bore area components, resurveying of the location of the end plug framework must be carried out in the Collision Hall, a space with little extra room to maneuver.

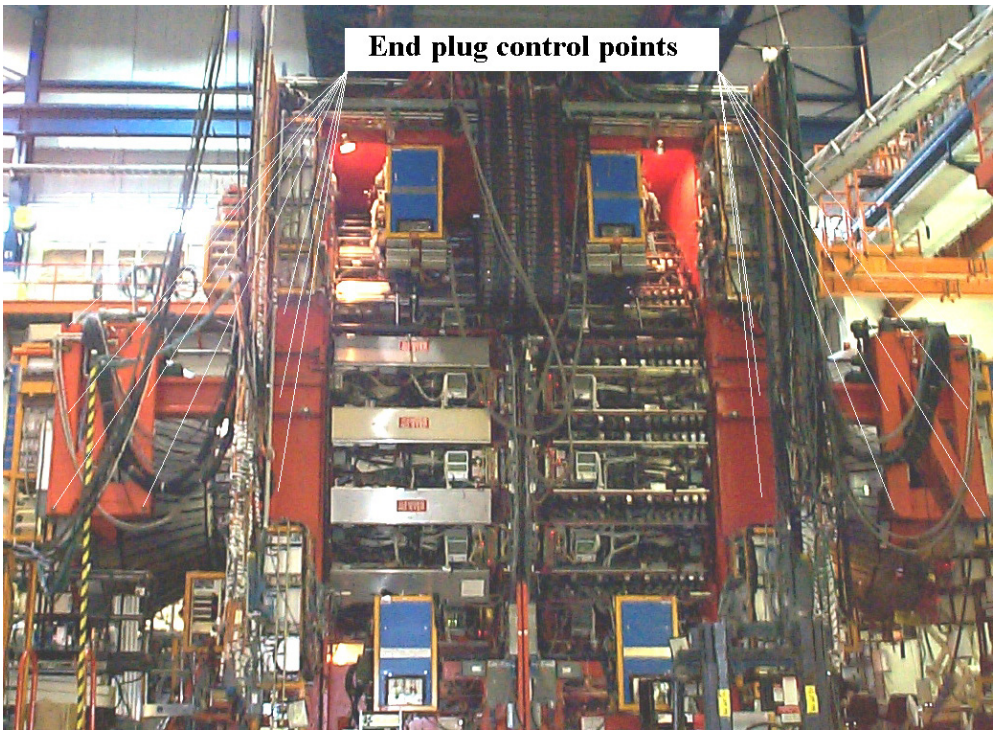

Figure 19 – End plug control

4. Laser Tracker + photogrammetry - adjustment and statistics

There are several strategies available for connecting dissimilar measurement schemes into a common network. These may include:

- Holding one system fixed, relative to the other
- Six-parameter transformations of one to the other
- Seven-parameter transformations of one to the other
- Developing observation equations for all data types
- Using the error estimates derived from the covariance matrix of a prior network for the points in common to constrain the connection

Laser Tracker networks are formed using observation equations for pseudo-slope distances, which in turn were formed from tracker-head coordinate data (3.1), and heights from digital leveling. The network may be constrained by fixed points or by the error estimates derived from covariance data.

In contrast, photogrammetry uses a ray-intersection method that derives great benefit from the potential for very large *degrees of freedom* figures. One of the primary benefits, beyond large redundancy for each measured point, is the ability to self-calibrate the camera system. This is done as an integral part of the bundle adjustment used to solve the photogrammetry network.

Being inherently scale-less, photogrammetry must be constrained by artifacts of known size or by a sufficient number of points for which a common reference frame is available. The knowledge of the point coordinates, a priori, may be fixed or applied with the estimates of the point errors.

Since error estimates are known from the Laser Tracker network adjustment (Table 10), the inclusion of these data can only serve to enhance the confidence in the photogrammetric results because the propagated error estimates will be more truly representative.

For this effort, three approaches were taken in order to assess the differences:

- Case I: A bundle solution with scale constraint, transformed with six-parameter Helmert transformation (Table 11)
- Case II: A bundle solution without scale constraint, using error estimates from the Laser Tracker network adjustment (Table 12)
- Case III: A bundle solution with scale constraint, using error estimates from the Laser Tracker network adjustment (Table 13)

Table 10 – AHLT coordinates (mm) and error estimates for points in common

Pt	X	Y	Z	δX	δY	δZ
ECLPLAT	-8192.66	-6084.50	-1479.25	0.18	0.06	0.13
HORZNE	-8680.49	-9703.39	-1722.72	0.17	0.08	0.14
HORZSE	-8026.83	-2423.97	-1721.33	0.14	0.08	0.30
NELPLAT	-8582.47	-9564.54	-1479.22	0.15	0.05	0.12
SELPLAT	-7954.53	-2571.74	-1475.58	0.18	0.06	0.16
TIESE	-7655.21	-2253.95	-1160.75	0.13	0.08	0.34
VS-5	-1131.93	-8821.36	3204.12	0.15	0.06	0.11
VS-6	-757.71	-4657.80	3202.81	0.13	0.06	0.10
VS-7	-749.67	-4663.37	1464.89	0.12	0.05	0.11
VS-8	-1127.59	-8813.79	1449.59	0.14	0.05	0.12

Table 11- Case I – using six-parameter transformation

Pt	dX	dY	dZ
ECLPLAT	0.039	-0.048	0.077
HORZNE	0.139	-0.051	-0.068
HORZSE	-0.065	-0.033	0.227
NELPLAT	0.137	-0.059	-0.063
SELPLAT	-0.059	-0.041	0.220
TIESE	-0.066	-0.046	0.231
VS-5	0.141	-0.041	-0.072
VS-6	0.024	-0.031	0.096
VS-7	0.015	0.041	0.096
VS-8	0.131	0.031	-0.072
RMS	0.057	0.060	0.081

Table 12 – Case II – using error estimates, without scale constraint

Pt	δX	δY	δZ
ECLPLAT	0.054	-0.290	0.030
HORZNE	-0.047	-0.241	0.078
HORZSE	-0.260	0.337	-0.228
NELPLAT	-0.005	-0.168	-0.001
SELPLAT	0.224	0.098	0.239
TIESE	-0.078	0.355	-0.144
VS-5	-0.157	-0.411	-0.040
VS-6	0.010	0.219	0.062
VS-7	0.135	0.355	0.031
VS-8	0.124	-0.254	-0.027
RMS	0.137	0.288	0.120

Table 13 – Case III – using error estimates, with scale constraint

Pt	δX	δY	δZ
ECLPLAT	0.147	-0.286	0.078
HORZNE	0.061	-0.122	0.134
HORZSE	-0.172	0.224	-0.172
NELPLAT	0.101	-0.052	0.047
SELPLAT	0.309	-0.010	0.287
TIESE	-0.003	0.237	-0.106
VS-5	-0.289	-0.320	-0.141
VS-6	-0.135	0.177	-0.039
VS-7	-0.010	0.313	-0.015
VS-8	-0.009	-0.162	-0.073
RMS	0.162	0.215	0.133

Cases I, II, and III (Tables 11, 12, and 13) represent successively more stringent criteria when considering error propagation. In Case I, the photogrammetric adjustment is considered a rigid body, which is simply "placed upon" the AHLT data, albeit a best-fit solution. Simple differences in coordinates are the only useful sense of precision. However, it may be argued that the coordinates of the photogrammetric data, derived by this method, are of value, just not the error estimates.

Case II allows the photogrammetric rays to "rattle around" within and about the error estimate envelope of the AHLT data. All scale information for the photogrammetric adjustment is derived solely from the AHLT data. The error estimates of these connections can be seen to degrade when compared with the approach of Case I (Table 12 compared to Table 11). The internal precision of the photogrammetric bundle, that is the RMS of all points adjusted in the bundle, not simply the connection points, which is a measure of the coherence of the solution was δX=0.060mm, δY=0.042mm, and δZ=0.034mm.

Case III uses an approach similar to that of Case II, but includes the Invar scale-bar data that was available in the images. The scale-bar, which carries retro-reflective targets on each end, measured 2.1336m +/- 0.0003m. It was located near the centroid of the photogrammetric network and approximately half way between the two clusters of AHLT data on the east and west faces of the CD. The comparison of Case II and Case III reveals only subtle differences in the RMS of the connection, as well as the internal precision (changing only in the fourth decimal

place). This latter observation indicates that the precision of the scale-bar was equivalent to that of the Laser Tracker.

The appropriate use of either Case II or Case III relies on the supposition that the control to which the photogrammetric data is connected, is well distributed within the volume of the network.

5. Collision Hall positioning of CD

After completion of the CD assembly, the CD was moved from the Assembly Hall to the Collision Hall. This is a very arduous task, requiring a large crew of people, several days to complete. Once the CD is in position to within a few centimeters, it was allowed to "rest" for several days in order to allow deformation of several millimeters to conclude.

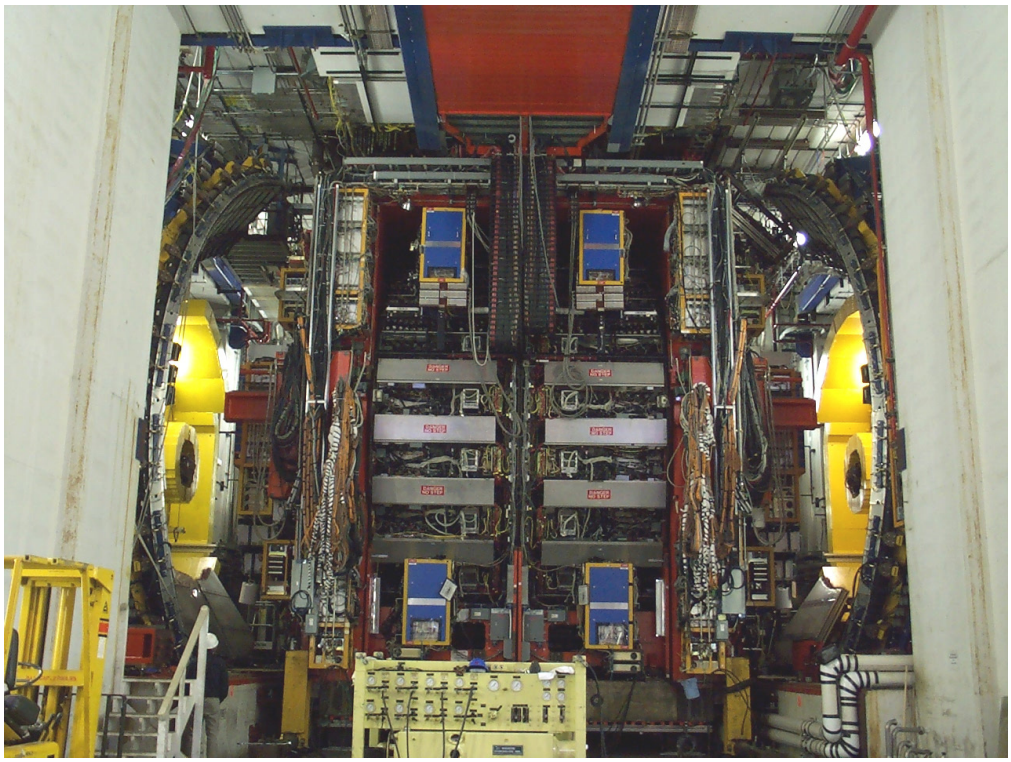

Figure 20 – Central Detector in Collision Hall

The coordinates of all components of the CD were transformed from the CD reference frame into the Collision Hall reference frame. Final positioning was accomplished by using two Laser Tracker systems, one located at the upstream face, the other at the downstream face (Figures 21 and 22). Each Laser Tracker was oriented in the Collision Hall reference frame. Four construction plates on the CD, two located on each face, were used to monitor the final movement of the CD. The four points lie at each corner of the CD, approximately in the same

plane. The Laser Tracker software has a "watch window" feature that allows the difference between actual coordinates and ideal coordinates to be monitored in real-time (Figures 23 and 24).

Figure 21 – SMX 3000 on west side

Figure 22 – SMX 4000 on east side

Figure 23 – SMR at control point

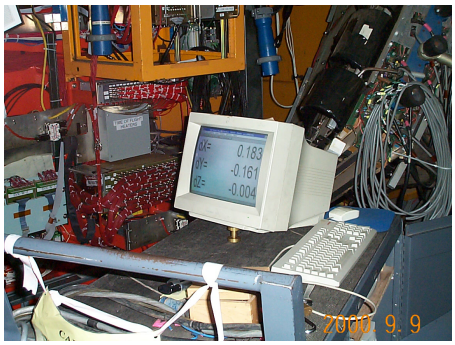

Figure 24 – Watch window

This feature provided instantaneous feedback to the rigging crew for their movement strategies, including calculation of shim-packs, translation components at both faces, and magnitude of the recoil reaction.

The difference, in millimeters, between the ideal positions and the as-built positions of the four control points were:

Table 14 – Summary of CD positioning data in Collision Hall

Pt	Horizontal	Vertical	Beam
NE	1.85	0.00	6.22
SE	1.90	-0.94	5.31
NW	1.63	-1.40	6.35
SW	1.78	-0.91	5.66
IP	1.68	-0.81	5.54

The as-built position of the interaction point (IP), calculated from the data, is shown in the table above. The roll, pitch, and yaw of the detector around the IP are -98μrad, -43μrad, and 32μrad, respectively. The internal precision, that is the Collision Hall Laser Tracker coordinates for the four CD control points, compared to the AHLT coordinates for those same points, yields an RMS fit of 0.249mm, 0.356mm, and 0.284mm. Factors contributing to these values are:

- Measurement error in the Collision Hall network
- Measurement error in the AHLT
- Measurement error from the two Laser Trackers fitting into the Collision Hall network and measuring to the CD
- Deformation of the Collision Hall in response to the installation of the CD
- Distortion of the CD as the result of the move from the Assembly Hall

6. Conclusions

The combined use of Laser Trackers, photogrammetry, and theodolite triangulation produced a network of superior quality, while taking advantage of each of these technologies' best capabilities. The preparation of the error estimates of the Laser Tracker network adjustment is straightforward, as is its inclusion in the photogrammetric bundle. The error propagation produced in either Case II or Case III is far more realistic than the six-parameter transformation.

7. Notation

The following notations are used in this paper

[1] V-STARS/S (Video-Simultaneous Triangulation And Resection System/Single camera)
[2] BETS (Brunson Electronic Theodolite System)
[3] DUSAF coordinate system is the traditional reference frame of the Tevatron, a NEU system.

8. References

Vanicek, P, Krakiwsky, E.J. (1986). *Geodesy The Concepts. 2nd Edition*, North-Holland Pub. Co., Amsterdam, 697 pp.

Wojcik G. J., Lakanen S. A. *The Adjustment of the Fermilab Main Injector Underground Geodetic Survey* Proceedings of the 5th International Workshops on Accelerator Alignment, Argonne National Laboratory, October 14-17, 1997